ORIGINAL PAPER

Differential Pharmacological Actions of Methadone and Buprenorphine in Human Embryonic Kidney 293 Cells Coexpressing Human μ-Opioid and Opioid Receptor-Like 1 Receptors

Cynthia Wei-Sheng Lee · Jia-Ying Yan · Yao-Chang Chiang · Tsai-Wei Hung · Hung-Li Wang · Lih-Chu Chiou · Ing-Kang Ho

Abstract Methadone and buprenorphine are used in maintenance therapy for heroin addicts. In this study, we compared their effects on adenylate cyclase (AC) activity in human embryonic kidney (HEK) 293 cells stably over-expressing human μ-opioid receptor (MOR) and nociceptin/opioid receptor-like 1 receptor (ORL1) simultaneously. After acute exposure, methadone inhibited AC activity; however, buprenorphine induced compromised AC inhibition. When naloxone was introduced after 30 min incubation with methadone, the AC activity was enhanced. This was not observed in the case of buprenorphine. Enhancement of the AC activity was more significant when the incubation lasted for 4 h, and prolonged exposure to buprenorphine elevated the AC activity as well. The removal of methadone and buprenorphine by washing also obtained similar AC superactivation as that revealed by naloxone challenge. The study demonstrated that methadone and buprenorphine exert initially different yet eventually convergent adaptive changes of AC activity in cells coexpressing human MOR and ORL1 receptors.

Keywords Opioid receptor · Adenylate cyclase activity · Morphine · Methadone · Buprenorphine · Naloxone

Introduction

Three conventional opioid receptors—μ (MOR), δ (DOR), and κ (KOR)—have been characterized based on their pharmacological, anatomical, and molecular properties [1–3]. A non-opioid branch of opioid receptors has also been identified and named as opioid receptor-like orphan receptor (ORL1) [4]. This receptor family was renamed after identification of its endogenous peptidergic agonist, nociceptin or orphanin FQ, as the nociceptin/orphanin FQ peptide (NOP) receptor; it displays pharmacology distinct from those of conventional opioid receptors [5, 6]. Activation of μ-, δ-, κ- or ORL1 receptor produces common cellular actions by regulating the same secondary messengers, including inhibition of adenylate cyclase (AC) activity [7, 8] and N-type [9] and L-type Ca^{2+} channels [10]. Activation of opioid receptors also increases phospholipase C activity, causes a transient increase in intracellular Ca^{2+} [11], and activates inwardly rectifying K^+ channels [12] and mitogen-activated protein kinases (MAPK) [13].

Methadone and buprenorphine are currently used in maintenance treatment programs for heroin addicts [14, 15]. Methadone is an orally available synthetic opioid functioning as a full agonist of MOR. First tested as a treatment for heroin addicts in early 1964 at The Rockefeller University,

C. W.-S. Lee · J.-Y. Yan · Y.-C. Chiang · T.-W. Hung · I.-K. Ho (✉)
Division of Mental Health and Addiction Medicine, Institute of Population Health Sciences, National Health Research Institutes, 35 Keyan Road, Zhunan, Miaoli County 35053, Taiwan
e-mail: iho@nhri.org.tw

H.-L. Wang
Department of Physiology, Chang Gung University School of Medicine, Kwei-San, Taoyuan 33302, Taiwan

L.-C. Chiou
Department of Pharmacology, College of Medicine, National Taiwan University, Taipei 10051, Taiwan

it provided a "blockade" against the effects of superimposed heroin through the mechanism of opioid cross-tolerance [14]. Buprenorphine, a derivative of thebaine, differs from standard opioid agonists in two aspects. The first is the slow receptor dissociation kinetics featured with the biphasic ("bell"- or "inverted U"-shaped) dose–response relation [16, 17]. The second is that buprenorphine has a ceiling effect on respiratory depression in humans, suggesting a greater safety margin of buprenorphine relative to other clinical opioids [18]. Methadone is a long-acting MOR agonist with pharmacological properties qualitatively similar to those of morphine, whereas buprenorphine is a MOR partial agonist and a potent κ-opioid receptor antagonist [19] as well as an ORL1 agonist [16, 20].

Adaptive changes in neurons underlie altered behaviors associated with opioid dependence and withdrawal syndrome [21]. Adaptations affect neuronal excitability, synaptic transmission, transcription factors, and MAPK [22]. Prolonged exposure of NG108-15 neuroblastoma x glioma hybrid cells (expressing mainly δ-opioid receptors) to morphine leads to increased AC activity [23], suggesting this phenomenon may underlie the withdrawal state. Withdrawal of the agonist by washing (natural withdrawal) or by adding the antagonist naloxone (precipitated withdrawal), which relieves the inhibition of AC exerted by the agonist, revealed the phenomenon of AC superactivation or overshoot. Such regulation of AC could be a general means of cellular adaption to the alteration of opioid receptors [24, 25].

In several subpopulations of CNS neurons involved in pain regulation, MOR and ORL1 are coexpressed [26, 27]. Furthermore, heterodimerization of MOR and ORL1 impairs the potency of MOR agonist [28] and attenuates ORL1-mediated inhibition of N-type channels [29]. Interestingly, mice lacking the ORL1 gene partially lose tolerance liability to morphine analgesia [30] and show marked attenuation of morphine-induced physical dependence, manifested as naloxone-precipitated withdrawal symptoms after repeated morphine treatments [31]. Hence, coexpressed MOR+ORL1 may reflect the native opioid receptors in some CNS regions and could provide the insight on the development of dependence on opioid drugs.

The human embryonic kidney (HEK) 293 cell line is a widely-distributed mammalian cell expression system and shares similar protein expression profiles with human neuronal cells [32]. In this study, we have established an in vitro cell model overexpressing human MOR and ORL1 individually or simultaneously in human embryonic kidney (HEK) 293 cells. Alterations of AC activity after acute or prolonged exposure to methadone and buprenorphine were compared in this model. Naloxone was utilized to demonstrate the specificity of the drugs and elicit the precipitated withdrawal. Effects of morphine and Ro 64-6198 were also examined as positive control for MOR and ORL1, respectively.

Experimental Procedure

Molecular Cloning of Human μ-Opioid and ORL1 Receptors

The full-length cDNA clones encoding the human MOR (Clone ID 30915262) and ORL1 receptor (Clone ID 5164017) were purchased from Open Biosystems (Huntsville, AL, USA). HA epitope (YPYDVPDYA) was added to the N-terminus of MOR with the aid of PCR amplification. Subsequently, cDNA of HA-tagged MOR was subcloned into a mammalian expression vector, pcDNA4/V5-His C (Invitrogen, Carlsbad, CA, USA), which is a zeocin-selectable vector [28]. The cDNA encoding ORL1 was subcloned into a mammalian expression vector, pCMV-Tag3 (Stratagene, La Jolla, CA, USA), which is a geneticin-selectable vector providing a myc tag (EQKLISEEDL) to the N-terminus. All sequences were verified by DNA sequence analysis.

Stable Expression of Human μ-Opioid and ORL1 Receptors in HEK 293 Cells

HEK 293 cells were grown in minimal essential medium (Invitrogen) supplemented with 10% fetal bovine serum, 100 units/ml penicillin, and 100 μg/ml streptomycin. Cell cultures were maintained at 37°C in a humidified 5% CO_2 incubator. The pcDNA4/V5-His C vector containing cDNA of HA-tagged human MOR or the pCMV-Tag3 vector containing cDNA of myc-tagged human ORL1 was transfected to HEK 293 cells by lipofection using FuGENE HD (Roche, Mannheim, Germany). Cell lines stably expressing HA-tagged MOR and myc-tagged ORL1 were selected by adding zeocin (0.5 mg/ml) and geneticin (0.5 mg/ml) to the culture medium, respectively. Surface expression of HA-tagged human MOR or myc-tagged human ORL1 was confirmed by measuring agonist-mediated inhibition of forskolin-induced cAMP accumulation [28].

Receptor Deglycosylation

HEK cells stably expressing MOR or ORL1 were grown to near confluence in 10 cm dishes. Cell extracts were prepared by incubating the cells in 0.4 ml of lysis buffer—composed of 150 mM Tris–HCl (pH 7.4), 300 mM NaCl, 1 mM $MgCl_2$, 1 mM $CaCl_2$, 1% Triton X-100, 10% glycerol, and 1% protease inhibitor mixture (containing aprotinin, leupeptin, pepstatin A, 4-(2-aminoethyl)benzenesulfonyl fluoride

hydrochloride, bestatin, and E-64; Sigma–Aldrich, St. Louis, MO, USA)—for 1 h on ice. Cell debris was precipitated by centrifugation at 14 000 g for 10 min at 4°C and the supernatant was used for the analysis. Protein concentration of the supernatant was determined using the BCA assay (Pierce Biotechnology, Rockford, IL, USA) with bovine serum albumin as standard. To investigate receptor glycosylation, 20 μg protein was incubated with 1 unit N-glycosidase F (Roche) in deglycosylation buffer—consisting of 25 mM sodium phosphate buffer (pH 7.2), 25 mM EDTA, 0.1% SDS, and 1% (v/v) 2-mercaptoethanol—at 37°C for 3 h [33]. For immunoblotting, treated and untreated lysates were diluted with 6× gel loading buffer (300 mM Tris–Cl (pH 6.8), 12% (w/v) SDS, 0.3% (w/v) bromophenol blue, 60% (v/v) glycerol, and 600 mM β-mercaptoethanol); and proteins were resolved using 10% SDS polyacrylamide gel and then transferred to polyvinylidene difluoride membranes (Immobilon; Millipore, Billerica, MA, USA). Membranes were incubated with monoclonal anti-HA or anti-myc antibody (1:1000 dilution; Cell Signaling Technology, Danvers, MA, USA) overnight at 4°C. After being washed, membranes were incubated with sheep anti-mouse horseradish peroxidase-linked secondary antibody (GE Healthcare Life Sciences, Piscataway, NJ, USA). Subsequently, immunoreactive proteins on the membrane were visualized by enhanced chemiluminescence (SuperSignal West Pico chemiluminescent substrate kit; Pierce Biotechnology, Rockford, IL, USA). Molecular weights were determined using ImageQuant TL (GE Healthcare Life Sciences).

Radioligand Binding Assays

HEK 293 cells were washed twice and harvested on ice in Versene solution containing 0.2 g/L EDTA•4Na in phosphate-buffered saline (Invitrogen) and centrifuged at 500 g for 3 min at 4°C. The cell pellet was suspended in buffer A—consisting of 5 mM Tris–Cl (pH 7.4), 5 mM EDTA, 5 mM EGTA, and 0.1 mM phenylmethylsulfonyl fluoride—passed through a 26-gauge 1/2 needle 5 times, and then centrifuged at 48 000 g for 30 min. The membrane pellet was resuspended using a Polytron homogenizer in buffer B—composed of 50 mM Tris–Cl (pH 7.0) and 0.32 mM sucrose—aliquoted, frozen in dry ice/ethanol, and stored at –80°C. Protein concentration of the membrane preparation was measured by the Bradford method (Bio-Rad protein assay kit, Bio-Rad Laboratories, Hercules, CA, USA).

Saturation radioligand binding assay was performed using opaque white 96-well filter plates with FB glass fiber filters (model MSFB N6B, Multiscreen Assay System; Millipore). Cell membranes (8 ~ 12 and 50 μg of protein/well for nociceptin and DAMGO binding, respectively)

were incubated with various concentrations of [³H]-nociceptin (PerkinElmer Life Analytical Sciences, Boston, MA, USA) or [³H]-DAMGO (PerkinElmer) in binding buffer consisting of 50 mM Tris–Cl (pH 7.4) and 1 mM EGTA for 1 h at 25°C. Non-specific binding was determined by adding 3 μM nociceptin (Tocris Bioscience, Ellisville, Missouri, USA) or DAMGO (Tocris) to the reaction mixture. The reaction was terminated by rapid filtration, and the filters were washed 3 times with ice-cold binding buffer and dried at room temperature, overnight. After adding MicroScint-20 cocktail (PerkinElmer), bound radioactivity was measured using the TopCount NXT microplate scintillation and luminescence counter (PerkinElmer). Prism (GraphPad Software, La Jolla, CA, USA) was used to analyze the data derived from the saturation binding assay to obtain B_{max} and K_D values.

Confocal Microscopy and Image Analysis

Cells were grown on microscope cover glasses (Fisher Scientific, Pittsburgh, PA, USA) and incubated for 2–3 days prior to immunocytochemistry. Immunostaining was performed by incubating the cells at 37°C with 1:100 dilution of monoclonal anti-HA (Cell Signaling Technology) or polyclonal anti-ORL1 (raised against the N-terminus of the human OPRL1 receptor, MEPLFPAPFWEVIYGSHL, and affinity-purified by Pro-Sci Incorporated, Poway, CA, USA) antibody in complete medium for 1.5 h. After three washes in complete medium and two washes in PBS⁺ (1 × phosphate-buffered saline containing 1 mM MgCl₂ and 0.1 mM CaCl₂), cells were fixed with 4% paraformaldehyde at room temperature for 15 min. After quenching with two washes with 50 mM NH₄Cl in PBS⁺ and washed once with PBS⁺, cells were permeabilized with 0.1% Triton X-100 in PBS⁺ at room temperature for 15 min. To remove excess Triton X-100, cells were washed 5 times with PBS⁺ at room temperature. Nonspecific binding was then blocked by incubating the cells with 10% BSA in PBS⁺ at room temperature for 30 min. The secondary antibody (1:500 dilution of Alexa Fluor 488 goat anti-mouse or Alexa Fluor 647 anti-rabbit antibody, Invitrogen) was applied at 4°C overnight. Cells were then washed 3 times with PBS⁺ and mounted (Pro-Long Gold Antifade Kit, Invitrogen) for imaging. Images were acquired using a Leica TCS SP5 confocal microscope (Leica Microsystems CMS GmbH, Mannheim, Germany) with a 63 × 1.4 NA oil immersion objective in the inverted configuration. Quantitative analysis of colocalization rate was performed using Leica LAS-AF software based on 30% background subtractions in both receptors and 30% threshold for determining colocalization.

HTRF cAMP Assays

The cAMP quantification was performed using a homogeneous time-resolved fluorescence (HTRF) cAMP detection kit (cAMP HiRange; Cisbio, Bagnols/Cèze Cedex, France). HEK 293 cells were dispensed with 25 µl of compound buffer consisted of minimal essential medium supplemented with 0.5 mM isobutylmethylxanthine (Sigma–Aldrich), 0.2% fatty acid-free bovine serum albumin (Sigma–Aldrich), 0.5 mg/ml zeocin, and/or 0.5 mg/ml geneticin at $2–6 \times 10^4$ cells/well in 96 half-well plates (Costar, Corning, NY, USA) on the day of the experiment. After an incubation of 1 h at 37°C in a humidified 5% CO_2 incubator, 25 µl of compound buffer containing 10 µM forskolin and desired concentrations of methadone (United States Pharmacopeia, Rockville, MD, USA) or buprenorphine (Sigma–Aldrich) were added to the cells, followed by 30 min incubation at room temperature. Morphine (National Bureau of Controlled Drugs, Taipei, Taiwan) and Ro 64-6198 (a gift from F. Hoffmann-La Roche Ltd., Basel, Switzerland)—which are a MOR agonist and an ORL1 agonist, respectively—were included as the positive control. Subsequently, 25 µl of cAMP-d2 and 25 µl of anti-cAMP Cryptate conjugate were added to each well. After 1 h incubation at room temperature, the plate was read on a FlexStation 3 microplate reader (Molecular Devices, Silicon Valley, CA, USA) with emission wavelength at 615 and 665 nm.

To verify the specificity of the drugs, 1 µM naloxone (Sigma–Aldrich) was included in the compound buffer containing 10 µM forskolin and 0.1 µM opioids, followed by 30 min co-incubation at room temperature. For evaluation of AC superactivation, desired concentrations of drugs were added to the compound buffer and incubated at 37°C for 30 min or 4 h; the compound buffer was then replaced by either 10 µM forskolin only or in combination with 1 µM naloxone. Afterward, the incubation with cAMP-d2 and anti-cAMP Cryptate conjugate was immediately carried out as stated above. The cAMP concentrations were calculated by nonlinear regression analysis with SoftMax Pro (Molecular Devices, Sunnyvale, CA, USA). Concentration-response curves of cAMP accumulation, potency (pIC_{50}) and efficacy (E_{max}) for inhibition of forskolin-stimulated cAMP formation by morphine, methadone, buprenorphine, and Ro 64-6198 were analyzed using Prism (GraphPad Software) [34, 35].

Statistical Analyses

All results are expressed as the mean ± SE value of n experiments. Paired/unpaired t test (two-tailed) or one-way/two-way ANOVA followed by Bonferroni's test was used to determine whether the difference is statistically significant ($P < 0.05$).

Results

Establishment of HEK 293 Cells Stably Expressing HA-Tagged MOR and Myc-Tagged ORL1

We have established an in vitro cell model by over-expressing epitope-tagged human MOR and ORL1 in HEK 293 cells. Plasmids harboring HA-tagged MOR or myc-tagged ORL1 were individually or simultaneously transfected in HEK 293 cells, and the stable clones were selected by appropriate antibiotics. Since adenylate cyclase (AC) activity is the major endpoint measured in this study, the three stable clones presented here (MOR-, ORL1-, and MOR+ORL1-expressing cells) were chosen based on the strongest adenylate AC inhibition by acute treatment of 1 µM of DAMGO and/or nociceptin compared to other stable clones during the initial screening. Subsequent experiments also demonstrated similar AC inhibition levels between the MOR- and MOR+ORL1-expressing cells or those between the ORL1- and MOR+ORL1-expressing cells elicited by MOR or ORL1 agonists (Fig. 3 and Table 2). Western blot analysis using monoclonal anti-HA antibody revealed that MOR was expressed as two major heterogeneous forms, with apparent molecular masses of ∼43–50 and 72–80 kilodaltons (kDa) (Fig. 1, Left panel). Due to its smaller mass, the ORL1 revealed by anti-myc antibody migrated more quickly as two major diffused bands with apparent molecular masses of ∼46–50 and 67–75 kDa. The minor band at ∼55 kDa is supposedly a non-specific protein elicited by overexpression of the plasmid harboring the myc-ORL1 receptor (Fig. 1, Right panel).

Since the apparent molecular weights of the overexpressed MOR and ORL1 were larger than the expected values, we hypothesized that the overexpressed human MOR and ORL1 might undergo glycosylation [2]. Evidence that MOR and ORL1 are glycoproteins was provided by digestion with N-glycosidase F, an amidase that cleaves nearly all types of N-glycan chains from the asparagines in N-linked glycoproteins. N-Glycosidase F treatment of MOR and ORL1 increased the mobility of both bands to species of apparent molecular masses of 43 kDa for MOR, and 39 and 41 kDa for ORL1. The predicted molecular masses for the HA-tagged MOR and myc-tagged ORL1 are ∼45 and 43 kDa, respectively. The reason for the aberrant electrophoretic mobility of the receptors, even after deglycosylation, is unknown at present [33]. The immunoreactive bands with slower mobility may represent opioid receptor dimers described previously [3, 36].

In saturation radioligand binding studies, [³H]-DAMGO displayed a similar affinity (K_D) for both stably transfected cell lines harboring MOR; but cells expressing MOR+ORL1 possess more DAMGO-binding sites than those expressing MOR alone, as reflected by the significantly higher B_{max}
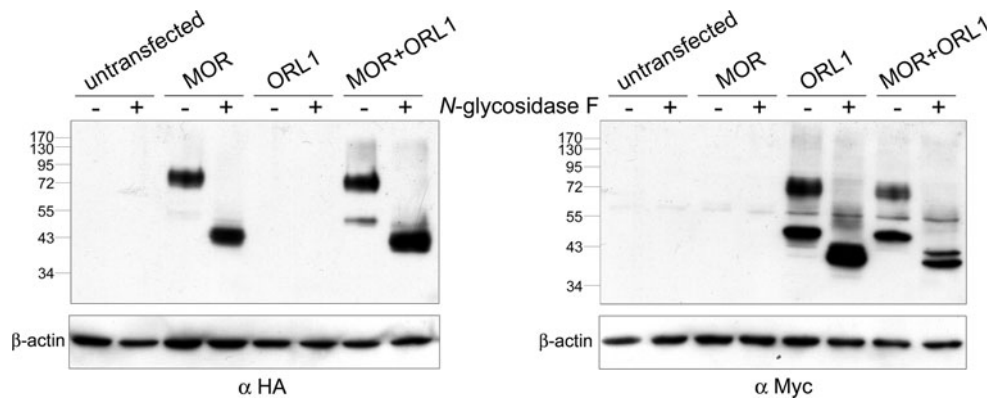
Fig. 1 MOR and ORL1 expressed in HEK 293 cells are *N*-linked glycoproteins. Cell lysates were prepared by extracting monolayers of HEK 293 cells expressing HA-tagged MOR and/or myc-tagged ORL1 receptors in lysis buffer for 1 h on ice. Cellular debris was pelleted by centrifugation; and the supernatants were treated with or without *N*-glycosidase F (protease-free, 50 units/mg of membrane protein) at 37°C for 3 h, then resolved using 10% SDS-PAGE. HA- or myc-tagged receptors were assayed by immunoblotting using the monoclonal anti-HA (*Left* panel) or anti-myc (*Right* panel) antibody. The mobilities of molecular mass standards (in kDa) are indicated to the left. -, glycosylated (untreated) receptors; +, deglycosylated (treated with *N*-glycosidase F) receptors

Table 1 B_{max} (pmol/mg protein) and K_D (nM) values of μ-opioid receptors (MOR) and opioid receptor-like 1 receptors (ORL1) expressed in HEK 293 cells

Receptor(s)	[³H]-DAMGO		[³H]-nociceptin	
	B_{max} (pmol/mg protein)	K_D (nM)	B_{max} (pmol/mg protein)	K_D (nM)
MOR	0.67 ± 0.07	5.25 ± 0.54		
ORL1			109.34 ± 54.11	2.83 ± 0.80
MOR+ORL1	$1.09 \pm 0.14^{\#}$	5.85 ± 0.72	17.38 ± 6.01	$0.69 \pm 0.20^{*}$

Saturation binding assays were performed with [³H]-DAMGO or [³H]-nociceptin. Each value represents the mean ± SE of four to five experiments performed in duplicate

[#] indicates the significant difference ($P < 0.05$) between B_{max} values of cells expressing only MOR and both MOR and ORL1

[*] indicates the significant difference ($P < 0.05$) between K_D values of ORL1-expressing cells and MOR+ORL1-expressing cells, according to unpaired *t* test (two-tailed) analysis

value (Table 1). In contrast, [³H]-nociceptin showed significantly higher affinity (lower K_D value) for cells expressing both MOR and ORL1 than cells expressing ORL1 alone; yet cells co-expressing MOR and ORL1 possess fewer nociceptin-binding sites than those expressing only ORL1, as demonstrated by the lower B_{max} value (Table 1).

We next examined whether MOR colocalizes with coexpressed ORL1. Shown in Fig. 2 are confocal fluorescence images of HEK 293 cells expressing HA-tagged MOR and myc-tagged ORL1. ORL1 was clearly present in vesicles distributed throughout the cytoplasm and also on the plasma membrane. MOR localizes to the cell surface as well as vesicular structures, and prominently colocalizes with ORL1 (colocalization rate: $83.65 \pm 4.33\%$).

AC Inhibition After Acute Opioid Exposure

Methadone Inhibited AC as a MOR Agonist

Effects of acute exposure to morphine, methadone, buprenorphine, and Ro 64-6198 on MOR- or ORL1-mediated Gα$_{i/o}$-coupled adenylate cyclase (AC) inhibition were examined. Morphine and methadone concentration-dependently inhibited forskolin-stimulated cAMP accumulation in HEK 293 cells expressing MOR only (Fig. 3a and b, open circles; Table 2) as well as MOR+ORL1 (Fig. 3a and b, filled squares; Table 2). Methadone was somewhat more potent than morphine in cells expressing only MOR (Table 2a) (pIC$_{50}$: 7.526 ± 0.127 vs. 6.702 ± 0.276) or MOR+ORL1 (Table 2b) (pIC$_{50}$: 7.294 ± 0.150 vs. 7.024 ± 0.193), although the difference is not statistically significant. In HEK 293 cells stably expressing ORL1, morphine and methadone did not inhibit forskolin-stimulated AC activity (Fig. 3a and b, open triangles). These results suggest that methadone acts as a potent MOR agonist comparable to morphine and has no effect on ORL1.

Buprenorphine Acted as an ORL1 Agonist and a Partial MOR Agonist

Unlike methadone, buprenorphine displayed a flat concentration-inhibition curve on cAMP accumulation in
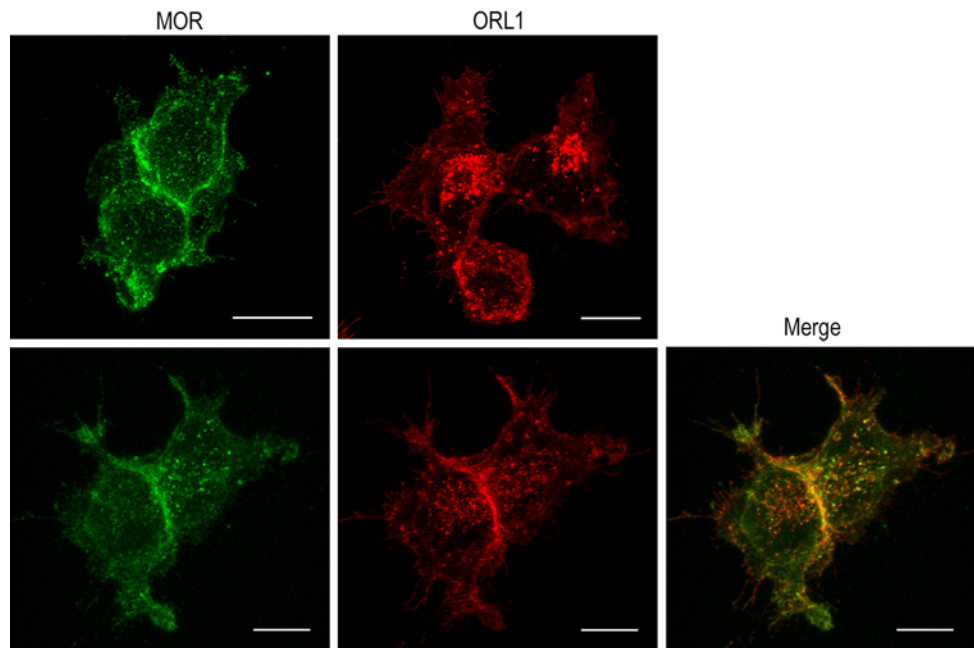
Fig. 2 Representative confocal images from cells expressing MOR (*Upper left* panel), ORL1 (*Upper right* panel), and MOR+ORL1 (*Lower* panels). HA-tagged MOR was detected with anti-HA mouse monoclonal antibody and visualized by Alexa Fluor 488 goat anti-mouse antibody (green); myc-tagged ORL1 was detected with anti- ORL1 rabbit polyclonal antibody and visualized by Alexa Fluor 647 goat anti-rabbit antibody (red); the colocalization of MOR and ORL1 is depicted in yellow in the merged picture. Scale bars are equal to 10 μm

MOR-expressing cells, with efficacy of only 33.52 ± 3.38% inhibition (Fig. 3c, open circles; Table 2), supporting its partial agonist characteristic at MOR. In ORL1-expressing cells, buprenorphine at higher concentrations (>30 nM) inhibited cAMP accumulation in a concentration-dependent manner (Fig. 3c, open triangles; Table 2), as did Ro 64-6198 (Fig. 3d, open triangles; Table 2), a non-peptide ORL1 agonist [37]. This suggests that buprenorphine acts as an ORL1 agonist at higher concentrations. Interestingly, buprenorphine showed a significantly greater potency (higher pIC_{50}) (Table 2c) but lower efficacy (lower E_{max}) (Table 2d) in MOR+ORL1-coexpressing cells than in cells expressing ORL1 only (Fig. 3c; Table 2). However, the AC inhibition curves elicited by Ro 64-6198 were comparable in ORL1- and MOR+ORL1-expressing cells (Fig. 3d; Table 2). This suggests that the effect of buprenorphine on MOR+ORL1-expressing cells is not solely owing to its agonistic property on ORL1 receptor.

Interactions of Naloxone

Naloxone, a generic opioid receptor antagonist, was co-incubated with 0.1 μM morphine, methadone and buprenorphine to verify if their effects were mediated by MOR. At 1 μM, naloxone did not affect forskolin-stimulated cAMP accumulation *per se* (nalox). However, it completely reversed the inhibitory effects of morphine and methadone; but it only slightly reversed the inhibitory effect of buprenorphine in cells expressing MOR (Fig. 4a) and MOR+ORL1 (Fig. 4b). Additionally, naloxone did not affect the Ro 64-6198-induced inhibition on cAMP accumulation (Fig. 4b and c), suggesting that naloxone at 1 μM specifically targets MOR and leaves ORL1 unaffected.

Naloxone, if added at the end of 30 min opioid exposure, relieved AC inhibition by morphine in cells expressing MOR or MOR+ORL1 and even caused a rebound facilitation of AC activity in the μM range (Fig. 5a). In cells treated with methadone, the AC activity was changed in a profile reminiscent of those exposed to morphine after naloxone challenge (Fig. 5b). Naloxone completely relieved buprenorphine-induced AC inhibition but did not induce rebound AC activity in cells expressing MOR and MOR+ORL1 (Fig. 5c). Interestingly, naloxone also significantly relieved the AC inhibition induced by buprenorphine at higher concentrations (Fig. 5c) as well as that induced by Ro 64-6198 (Fig. 5d) in ORL1-expressing cells. These results demonstrate that naloxone relieved AC inhibition induced by MOR agonists (morphine, methadone, and buprenorphine) and even induced rebound AC activity after 30 min exposure to higher concentrations of MOR agonists (morphine and methadone) but not after similar exposure to a partial agonist (buprenorphine). Naloxone also partially relieved the AC inhibition induced by ORL1 agonists, buprenorphine (Fig. 5c) and Ro 64-6198 (Fig. 5d), at higher concentrations in ORL1-expressing cells.
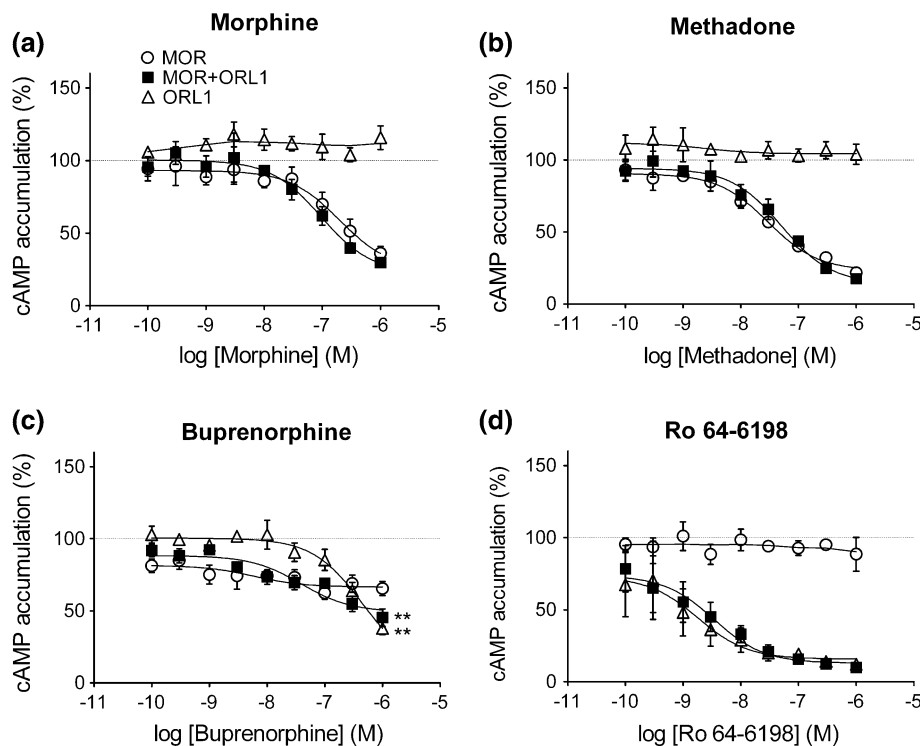
Fig. 3 Effects of acute exposures to morphine, methadone, bupr-enorphine, or Ro 64-6198 on forskolin-stimulated cAMP accumulation in HEK 293 cells expressing MOR and/or ORL1. HEK 293 cells expressing MOR (*open circle*), ORL1 (*open triangle*) or both MOR and ORL1 (*filled square*) were treated with morphine (**a**), methadone (**b**), buprenorphine (**c**), or Ro 64-6198 (**d**) for 30 min at room temperature in the presence of 10 μM forskolin prior to HTRF cAMP assays. Each point represents the mean ± SE value of four experiments performed in duplicate using different batches of cells. 100% defines forskolin-stimulated cAMP accumulation in cells not treated with aforementioned drugs. *Asterisks* in (**c**) indicate the very significant difference ($P < 0.01$) between curves of ORL1-expressing cells and MOR+ORL1-expressing cells according to paired *t* test (two-tailed) analysis

Table 2 Potency (pIC$_{50}$) and efficacy (E_{max}) for inhibition of forskolin-stimulated cAMP formation by morphine, methadone, buprenorphine, and Ro 64-6198 in HEK 293 cells expressing μ-opioid receptors (MOR) and opioid receptor-like 1 receptors (ORL1)

Drug	Receptor(s)	pIC$_{50}$	E_{max} (% inhibition)
Morphine	MOR	6.702 ± 0.276[a]	75.44 ± 13.97
	MOR+ORL1	7.024 ± 0.193[b]	77.54 ± 9.03
	ORL1	N/C	N/C
Methadone	MOR	7.526 ± 0.127[a]	76.79 ± 3.99
	MOR+ORL1	7.294 ± 0.150[b]	85.89 ± 6.24
	ORL1	N/C	N/C
Buprenorphine	MOR	8.224 ± 0.645	33.52 ± 3.38
	MOR+ORL1	7.412 ± 0.227*[c]	50.84 ± 4.37[d]
	ORL1	6.346 ± 0.214*[c]	90.51 ± 18.66[d]
Ro 64-6198	MOR	N/C	N/C
	MOR+ORL1	8.465 ± 0.270	87.10 ± 5.16
	ORL1	8.746 ± 0.422	84.27 ± 6.67

Values represent the mean ± SE of four experiments performed in duplicate as described in Fig. 3

* indicates a significant difference ($P < 0.05$) between the pIC$_{50}$ value of ORL1-expressing cells and that of MOR+ORL1-expressing cells, according to two-way ANOVA with Bonferroni correction. N/C = not converged. Lowercase letters (a–d) denote the points of comparisons described in the text
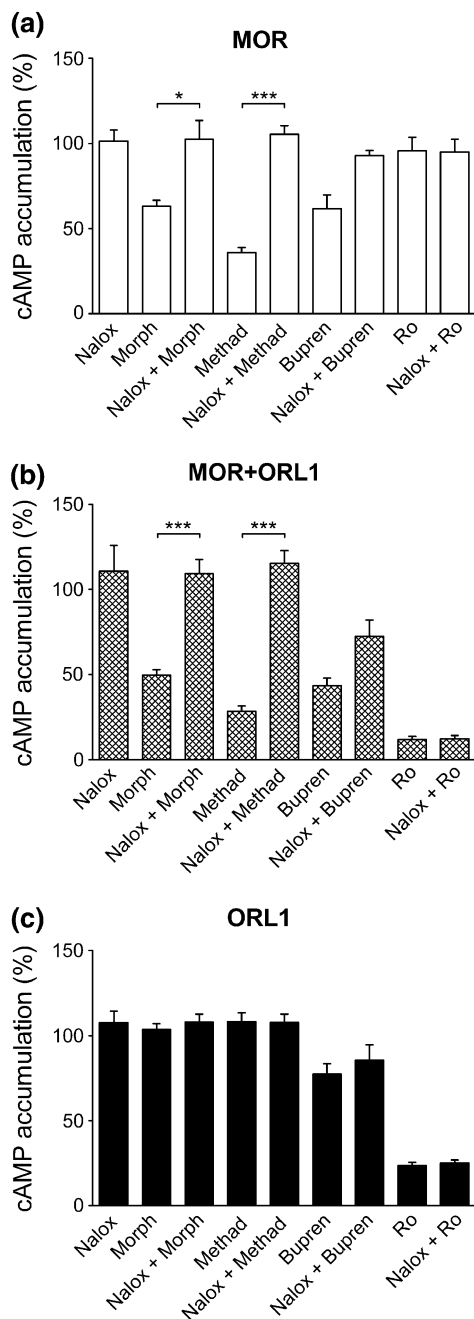
Fig. 4 Blockade by naloxone of the morphine, methadone, and buprenorphine inhibition on forskolin-stimulated cAMP accumulation in HEK 293 cells expressing MOR and/or ORL1. HEK 293 cells expressing MOR (**a**), MOR+ORL1 (**b**), or ORL1 (**c**) were treated with 0.1 μM morphine (morph), methadone (methad), buprenorphine (bupren), or Ro 64-6198 (Ro) in the presence or absence of 1 μM naloxone (nalox) for 30 min at room temperature with 10 μM forskolin prior to HTRF cAMP assays. Each point represents the mean ± SE value of four experiments performed in duplicate using different batches of cells. 100% defines forskolin-stimulated cAMP accumulation in cells not treated with aforementioned drugs. The significance of differences between without and with naloxone treatment were determined by one-way ANOVA followed by Bonferroni's test, *$P < 0.05$, ***$P < 0.001$

AC Superactivation After Chronic Opioid Treatment

AC Superactivation After Naloxone Challenge Following Long-Term Opioid Exposure

The above results show that rebound AC activity can be induced by naloxone in cells exposed to MOR agonists for only 30 min. Accordingly, we extended our investigation by adding naloxone to cells exposed to opioids for 4 h, an incubation period reported to show a prominent overshoot in forskolin-stimulated cAMP accumulation [38].

When HEK 293 cells expressing MOR and MOR+ ORL1 were exposed to morphine or methadone for 4 h, addition of naloxone caused AC superactivation, as revealed by the overshoot (up to 400%) of cAMP accumulation (Fig. 6a and b). However, no AC superactivation was observed in MOR-expressing cells chronically exposed to buprenorphine (Fig. 6c) or Ro 64-6198 (except at > 0.3 μM) (Fig. 6d) after naloxone challenge. Interestingly, AC superactivation did occur in ORL1- and MOR+ORL1-expressing cells chronically exposed to buprenorphine, and ORL1-expressing cells even exhibited larger magnitude of AC superactivation than MOR+ ORL1-expressing cells, as shown in the higher slope value in linear regression analysis (Fig. 6c). Chronic treatment with Ro 64-6198 also responded to naloxone "precipitation" and resulted in AC superactivation in cells expressing ORL1, both individually and simultaneously, with intriguingly bell-shaped concentration-response curves and higher efficacy in cells coexpressing MOR and ORL1 (Fig. 6d).

AC Superactivation After Agonist Removal Following Long-Term Opioid Exposure

Since naloxone does not act on ORL1 (Fig. 4) yet cells stably expressing ORL1 showed AC superactivation upon addition of naloxone (Fig. 6c and d), we investigated whether removal of agonist is sufficient to reveal AC superactivation after prolonged agonist exposure. Indeed, both buprenorphine and Ro 64-6198 resulted in AC superactivation (sixfold and 2.5-fold increases for buprenorphine and Ro 64-6198, respectively) after agonist removal in cells expressing solely ORL1 (Fig. 7c and d). Not surprisingly, morphine and methadone were still able to stimulate AC superactivation, yet to a lesser extent, in cells expressing MOR and MOR+ORL1 in the absence of naloxone challenge (Fig. 7a and b). Hence, we demonstrated that "natural withdrawal" by washout (Fig. 7) and "precipitated withdrawal" by naloxone (Fig. 6) have similar effects on cAMP accumulation; additionally, chronic exposure to buprenorphine and Ro 64-6198 could also contribute to the "withdrawal syndrome" (i.e. AC
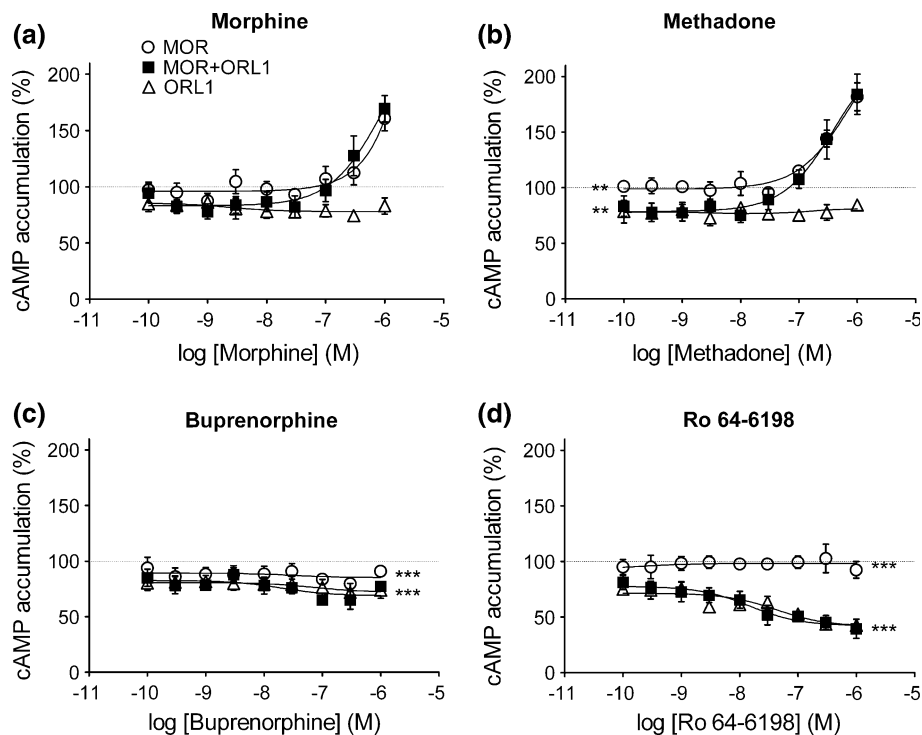
Fig. 5 Effects of naloxone on acute exposures to morphine, methadone, buprenorphine, or Ro 64-6198 on forskolin-induced cAMP accumulation in HEK 293 cells expressing MOR and/or ORL1. After exposure to morphine (**a**), methadone (**b**), buprenorphine (**c**), or Ro 64-6198 (**d**) for 30 min at room temperature, the incubation media were subsequently removed, and HEK 293 cells expressing MOR (*open circle*), ORL1 (*open triangle*) or both MOR and ORL1 (*filled square*) were treated with 1 μM naloxone accompanied by 10 μM forskolin immediately prior to HTRF cAMP assays. Each point represents the mean ± SE value of four experiments performed in duplicate using different batches of cells. 100% defines forskolin-stimulated cAMP accumulation in cells treated with none of the aforementioned drugs but naloxone. *Asterisks* indicate the significant differences (**$P < 0.01$, ***$P < 0.001$) between curves of MOR-expressing cells and MOR+ORL1-expressing cells according to paired *t* test (two-tailed) analysis

superactivation) in cells expressing ORL1 in our in vitro cell model.

Discussion

Heterodimerization of MOR-ORL1

Heterodimerization has been reported for MOR and various receptors, such as the δ opioid receptor [39], ORL1 receptor [28], sst$_{2A}$ somatostatin receptor [40], substance P receptor [41], cannabinoid CB$_1$ receptor [42], and metabotropic glutamate receptor 5 [43]. Receptor heterodimerization usually leads to alterations in MOR phosphorylation, internalization, desensitization, MAPK activation, and coupling to voltage-dependent Ca^{2+} channels [44]. We demonstrated the colocalization of coexpressed human MOR and ORL1 receptors in HEK 293 cells (Fig. 2). Although the colocalization rate did not reach 100%, indicating the presence of homomers in the coexpressed condition, the high colocalization rate suggests the formation of heterodimerized MOR-ORL1 as recently reported in tsA-201 cell [29]. We attempted to co-immunoprecipitate the coexpressed human MOR and ORL1 using anti-HA and anti-myc antibodies, but were unable to detect the direct association of MOR and ORL1 by pulling down the receptors together. Hence, human MOR and ORL1 may indeed heterodimerize but cannot be co-immunoprecipitated, or co-immunoprecipitation with the anti-N-terminal epitope tags is unable to detect the association of human MOR and ORL1. Our saturation binding assay using [^{3}H]-nociceptin (Table 1)—which showed that co-expressing ORL1 with MOR reduced the number of nociceptin-binding sites (lower B_{max}) yet significantly increased the nociceptin affinity of the receptor (lower K_D)—also implies the novel properties of coexpressed human MOR-ORL1 receptors. This interesting phenomenon was not seen in HEK 293 cells co-expressing rat MOR and ORL1 [28]. Since the expression levels of myc-tagged ORL1 are not drastically different in cells expressing ORL1 alone and MOR+ORL1 as revealed by immunoblotting (Fig. 1), the reduction of B_{max} might be due to the decreased number of ORL1 transported from ER-Golgi to the plasma membrane [45]. Another possibility is that coexpressed human MOR and ORL1, perhaps forming heteromers, adopted a different
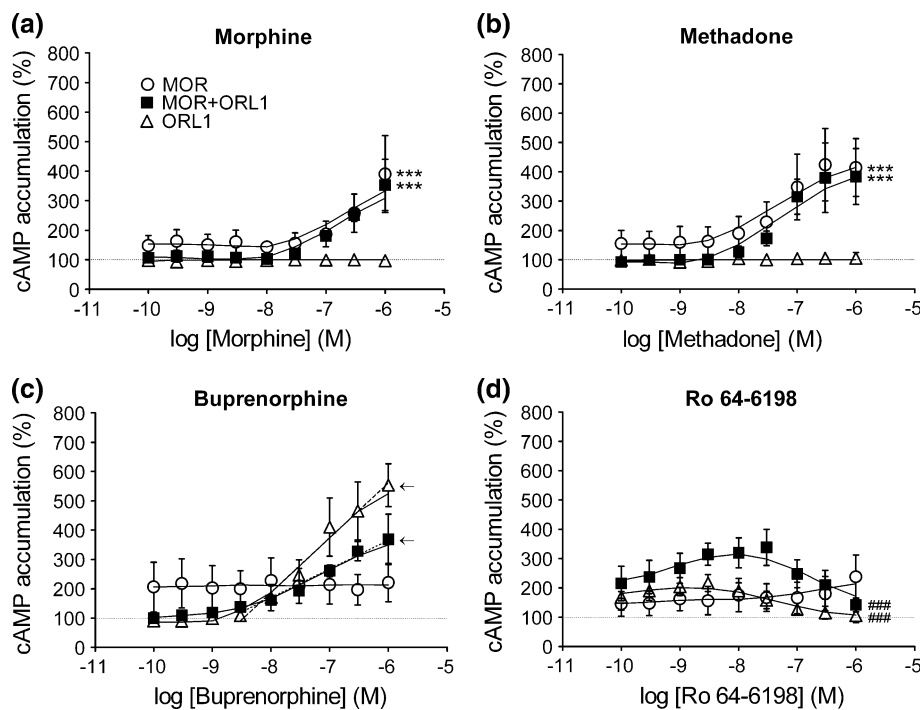
Fig. 6 Naloxone precipitation on the effects of chronic exposures to morphine, methadone, buprenorphine, or Ro 64-6198 on forskolin-stimulated cAMP accumulation in HEK 293 cells expressing MOR and/or ORL1. HEK 293 cells expressing MOR (*open circle*), ORL1 (*open triangle*) or both MOR and ORL1 (*filled square*) were treated with morphine (**a**), methadone (**b**), buprenorphine (**c**), or Ro 64-6198 (**d**) for 4 h at 37°C. The incubation medium was subsequently replaced by 1 μM naloxone and 10 μM forskolin in compound buffer prior to HTRF cAMP assays. Each point represents the mean ± SE value of four experiments performed in duplicate using different batches of cells. 100% defines forskolin-stimulated cAMP accumulation in cells not treated with aforementioned drugs. *Asterisks* indicate the extremely significant differences ($P < 0.001$) between curves of cells expressing MOR alone (*open circle*) and both MOR and ORL1 (*filled square*). *Pound signs* indicate the extremely significant difference ($P < 0.001$) between curves of cells expressing only ORL1 (*open triangle*) and both MOR and ORL1 (*filled square*) according to paired t test (two-tailed) analysis. *Dashed* and *dotted* lines represents the linear regression fitted to the 6 data points at the high concentration end of cells expressing ORL1 (*open triangle*; slope = 186.4 ± 30.82) and both MOR and ORL1 (*filled square*; slope = 97.80 ± 17.31), respectively. *Arrows* indicate the significant difference ($P < 0.05$) between the slopes of the linear regression

conformation of the nociceptin-binding site from ORL1, rendering the binding affinity higher than ORL1 homomers [43, 46]. A potential caveat of the overexpression system is that the interaction between two overexpressed receptors might be mass action-induced and does not exist in endogenous system where the receptor abundance is much lower. Therefore, our in vitro cell model is a simplified system to address the possible heterodimerization between MOR and ORL1, and may not truthfully reflect the native condition of these two opioid receptors in the in vivo system.

Acute activation of MOR and ORL1 Inhibits AC Activity

Acute agonist exposure inhibits forskolin-induced accumulation of cAMP in recombinant HEK 293 cells expressing cloned MOR [47] or ORL1 [48]; this effect is mediated by inhibition of AC activity upon opioid receptor activation [49, 50]. In our cell model, acute treatment with two MOR agonists, morphine and methadone, specifically repressed the AC activity in cells expressing recombinant MOR. The ORL1 agonist, Ro 64-6198, acutely inhibited AC in cells expressing recombinant ORL1 but not MOR alone. Buprenorphine, which acted as a partial agonist at MOR and as a full agonist at ORL1, exhibited an intermediate potency (pIC_{50}) and efficacy (E_{max}) in cells coexpressing MOR and ORL1 in comparison to MOR or ORL1 alone (Table 2). This intermediate response might result from the heterodimerization of MOR and ORL1, or the simultaneous regulation of common secondary messengers by MOR and ORL1.

Changes in the cAMP system in the locus coeruleus (LC) play a role in mediating acute opioid action and underlying the development of opioid dependence and withdrawal [51]. Morphine acutely inhibited AC in vitro in the LC, dorsal raphe, frontal cortex, and neostriatum; and the inhibition was blocked by naloxone. This response is mediated by a pertussis toxin-sensitive G-protein (i.e. $G_{i/o}$) [51]. We successfully replicated the phenomenon in the in
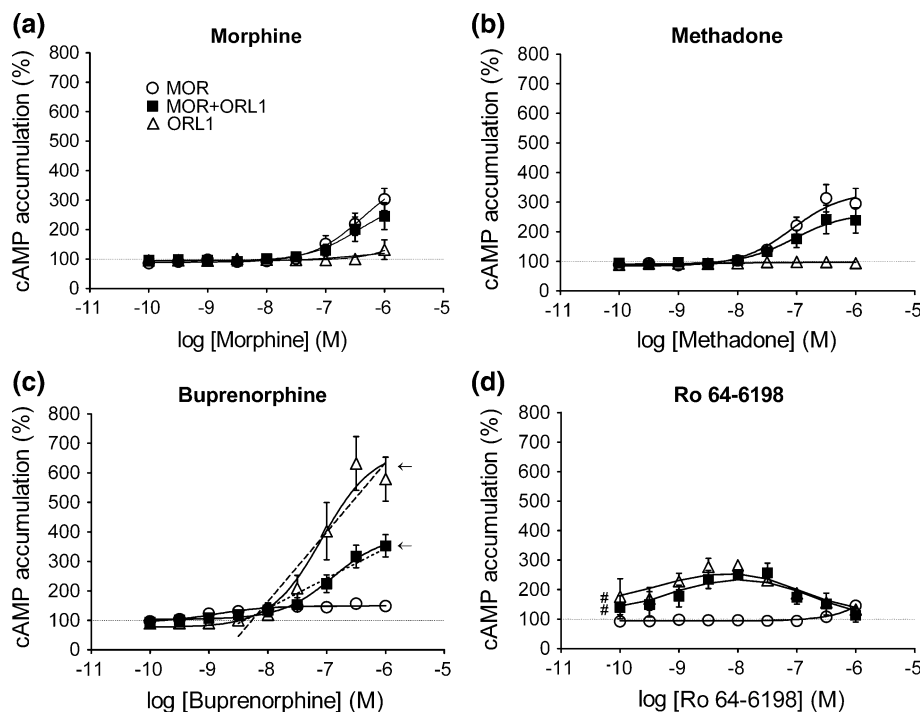
Fig. 7 "Natural withdrawal" on the effects of chronic exposures to morphine, methadone, buprenorphine, or Ro 64-6198 on forskolin-stimulated cAMP accumulation in HEK 293 cells expressing ORL1 and/or MOR. HEK 293 cells expressing MOR (*open circle*), ORL1 (*open triangle*) or both MOR and ORL1 (*filled square*) were treated with morphine (**a**), methadone (**b**), buprenorphine (**c**), or Ro 64-6198 (**d**) for 4 h at 37°C. The incubation medium was subsequently replaced by 10 μM forskolin in compound buffer prior to HTRF cAMP assays. Each point represents the mean ± SE value of four experiments performed in duplicate using different batches of cells. 100% defines forskolin-stimulated cAMP accumulation in cells not treated with aforementioned drugs. *Dashed* and *dotted* lines represents the linear regression fitted to the six data points at the high concentration end of cells expressing ORL1 (*open triangle*; slope = 235.8 ± 32.62) and both MOR and ORL1 (*filled square*; slope = 101.9 ± 13.89), respectively. *Arrows* indicate the extremely significant difference ($P < 0.001$) between the slopes of the linear regression. *Pound signs* indicate the significant difference ($P < 0.05$) between curves of cells expressing only ORL1 (*open triangle*) and both MOR and ORL1 (*filled square*) according to paired t test (two-tailed) analysis

vitro cell model: morphine acutely inhibited AC in HEK 293 cells overexpressing MOR and MOR+ORL1 (Fig. 3a); and the inhibition was also blocked by naloxone (Fig. 3a and b). Acute exposure to agonists of $G_{i/o}$-coupled receptors—such as MOR, m_4 (muscarinic type 4), D_2 (dopaminergic type 2), and CB_1 (cannabinoid type 1) receptors—inhibits the activity of AC types I, V, VI, and VIII, while stimulating the activity of AC types II, IV, and VII [25, 52]. Furthermore, acute activation of $G_{i/o}$-coupled receptors leads to inhibition of AC-VIII-A and -B, but not of the AC-VIII-C splice variant in COS-7 cells transfected with MOR [53]. It would be interesting to investigate whether the cells coexpressing MOR and ORL1 utilize the same mechanism to regulate AC activity as well.

AC Superactivation After Chronic Agonist Treatment

Opioid-induced AC superactivation has been widely used as an indicator of cellular dependence [54]. Cell lines expressing either MOR or ORL1 have been successfully utilized to investigate the overshoot of AC activity

following chronic treatment of agonists [38, 55]. The present study further used cells co-expressing MOR and ORL1 and observed unique responses of the coexpressed MOR+ORL1 receptors, which suggests that coexpressed MOR+ORL1 receptors perhaps represent a distinct population of the opioid receptors: ones that bear pharmacological profiles different from either MOR or ORL1 alone. Our results demonstrated that the AC superactivation could start as early as 30 min after morphine or methadone treatment (Fig. 5a and b); and 4 h incubation with the MOR agonist resulted in profound AC superactivation either in the presence of naloxone challenge (Fig. 6) or simply after agonist washout (Fig. 7).

The LC nucleus possesses a high density of opioid receptors, particularly MOR [56] and ORL1 [57]. Chronic morphine administration elevates levels of AC-I and AC-VIII in the LC [58] and knockout of either calmodulin-dependent isoform attenuates the ability of chronic morphine exposure to increase LC neuronal excitability and behavioral features of opioid withdrawal [59]. Blockade of cAMP response-element binding protein (CREB) in the LC

prevents the opioid-induced AC-VIII up-regulation [58]. Such blockade also diminishes the ability of chronic morphine treatment to increase LC neuronal excitability and to induce dependence and withdrawal [58, 60]. An ex vivo LC slice culture system combined with viral-mediated gene transfer and genetic mutant mice provides direct evidence supporting that prolonged morphine exposure induces homeostatic adaptations intrinsic to LC neurons, involving up-regulation of cAMP-CREB pathway, which enhances LC neuronal excitability [61]. Given the colocalization of MOR and ORL1 in the LC and our HEK 293 cells (Fig. 2), the present in vitro cell model expressing MOR+ORL1 offers the opportunity to dissect, in a simplified and more accessible manner, the relationship among MOR, ORL1, AC-I, AC-VIII, cAMP-CREB, and cell excitability during chronic exposure to morphine, methadone, and buprenorphine.

AC Superactivation Induced by Buprenorphine and Ro 64-6198 at ORL1

Although buprenorphine did not elicit AC superactivation at the 30 min time point (Fig. 5c), 4 h buprenorphine exposure induced prominent forskolin-induced cAMP accumulation ($\sim$3.5 fold) in MOR+ORL1-expressing cells and drastically high cAMP accumulation ($\sim$sixfold) in ORL1-expressing cells (Figs. 6c and 7c). Another striking observation is the bell-shaped curve of Ro 64-6198-induced AC superactivation (Figs. 6d and 7d). This biphasic response might reflect an intrinsic ORL1 property that receptor activation by higher concentration (above 0.1 μM) of agonists would generate a reduction, not an enhancement, of AC superactivation, thus contributing to its role in modulating opioid antinociception [62] and blocking the rewarding effects of several abused drugs, including morphine [63], cocaine [64], and amphetamine [65]. The difference between buprenorphine and Ro 64-6198 remains to be elucidated if it is due to the difference between the partial agonist (buprenorphine) and full agonist (Ro 64-6198) for ORL1.

Clinical Implications

When the responses to long-term treatment of methadone and buprenorphine are compared, cells expressing both MOR and ORL1 display matching concentration-response curves (Fig. 6b and c; Fig. 7b and c, filled squares). In contrast, cells expressing MOR alone concentration-dependently responded to methadone, not to buprenorphine (Fig. 6b and c; Fig. 7b and c, open circles), whereas ORL1-expressing cells exhibited concentration-dependent response to buprenorphine but not to methadone (Fig. 6b and c; Fig. 7b and c, open triangles). This implies that

chronic methadone and buprenorphine treatments induce differential effects on cells expressing either MOR or ORL1 alone, yet lead to similar cellular responses in the context of coexpressed MOR and ORL1. Therefore, our cellular model could mimic the physiological responses of patients, expressing both MOR and ORL1, under maintenance therapy.

The temporal difference between spontaneous and precipitated withdrawal might be explained by our cell model, revealing that naloxone-precipitated withdrawal (Fig. 6) elicited more prominent AC superactivation than natural withdrawal (Fig. 7) after chronic opioid exposure. Moreover, naloxone produces "overshoot" phenomena suggestive of early acute physical dependence 6–24 h after a single dose of a MOR agonist [66]. This acute physical dependence is reflected in the elevated AC activity precipitated by naloxone in MOR-expressing cells after 30 min exposure to morphine and methadone (Fig. 5a and b). Thus, our study provides a clue to the cellular mechanism of the opioid withdrawal precipitated by naloxone.

In summary, our study suggests that methadone and buprenorphine exert different adaptive changes on the secondary messengers. While methadone and morphine bear almost indistinguishable pharmacological profiles in AC superactivation after chronic treatment, buprenorphine carries a dissimilar pharmacological portrait, presumably originating from its agonistic function to ORL1. The in vitro cell model of coexpressed human MOR+ORL1 receptors provides insight into cross-talk between opioid receptors following prolonged opioid exposure, and could provide a new approach to examining novel drugs prior to their clinical use and an uncomplicated tool for investigating related signaling pathways of opioids at the cellular level.

References

1. Dhawan BN, Cesselin F, Raghubir R et al (1996) International union of pharmacology. XII. Classification of opioid receptors. Pharmacol Rev 48:567–592

2. Satoh M, Minami M (1995) Molecular pharmacology of the opioid receptors. Pharmacol Ther 68:343–364

3. Alfaras-Melainis K, Gomes I, Rozenfeld R et al (2009) Modulation of opioid receptor function by protein–protein interactions. Front Biosci 14:3594–3607

4. Mollereau C, Parmentier M, Mailleux P et al (1994) ORL1, a novel member of the opioid receptor family. Cloning, functional expression and localization. FEBS Lett 341:33–38

5. Chiou LC, Liao YY, Fan PC et al (2007) Nociceptin/orphanin FQ peptide receptors: pharmacology and clinical implications. Curr Drug Targets 8:117–135

6. Connor M, Christie MD (1999) Opioid receptor signalling mechanisms. Clin Exp Pharmacol Physiol 26:493–499

7. Evans CJ, Keith DE Jr, Morrison H et al (1992) Cloning of a delta opioid receptor by functional expression. Science 258:1952–1955

8. Meng F, Xie GX, Thompson RC et al (1993) Cloning and pharmacological characterization of a rat kappa opioid receptor. Proc Natl Acad Sci USA 90:9954–9958

9. Tallent M, Dichter MA, Bell GI et al (1994) The cloned kappa opioid receptor couples to an N-type calcium current in undifferentiated PC-12 cells. Neuroscience 63:1033–1040

10. Piros ET, Prather PL, Law PY et al (1996) Voltage-dependent inhibition of Ca^{2+} channels in GH3 cells by cloned mu- and delta-opioid receptors. Mol Pharmacol 50:947–956

11. Spencer RJ, Jin W, Thayer SA et al (1997) Mobilization of Ca^{2+} from intracellular stores in transfected neuro2a cells by activation of multiple opioid receptor subtypes. Biochem Pharmacol 54:809–818

12. Ikeda K, Kobayashi K, Kobayashi T et al (1997) Functional coupling of the nociceptin/orphanin FQ receptor with the G-protein-activated K^+ (GIRK) channel. Brain Res Mol Brain Res 45:117–126

13. Fukuda K, Kato S, Morikawa H et al (1996) Functional coupling of the delta-, mu-, and kappa-opioid receptors to mitogen-activated protein kinase and arachidonate release in Chinese hamster ovary cells. J Neurochem 67:1309–1316

14. Kreek MJ, LaForge KS, Butelman E (2002) Pharmacotherapy of addictions. Nat Rev Drug Discov 1:710–726

15. Haasen C, van den Brink W (2006) Innovations in agonist maintenance treatment of opioid-dependent patients. Curr Opin Psychiatry 19:631–636

16. Lutfy K, Eitan S, Bryant CD et al (2003) Buprenorphine-induced antinociception is mediated by mu-opioid receptors and compromised by concomitant activation of opioid receptor-like receptors. J Neurosci 23:10331–10337

17. Christoph T, Kogel B, Schiene K et al (2005) Broad analgesic profile of buprenorphine in rodent models of acute and chronic pain. Eur J Pharmacol 507:87–98

18. Dahan A, Yassen A, Romberg R et al (2006) Buprenorphine induces ceiling in respiratory depression but not in analgesia. Br J Anaesth 96:627–632

19. Gutstein HB, Akil H (2001) Opioid analgesics. In: Goodman LS, Hardman JG, Limbird LE et al (eds) Goodman & Gilman's the pharmacological basis of therapeutics. McGraw-Hill, Medical Pub. Division, New York, pp 569–619

20. Bloms-Funke P, Gillen C, Schuettler AJ et al (2000) Agonistic effects of the opioid buprenorphine on the nociceptin/OFQ receptor. Peptides 21:1141–1146

21. Weiss F (2005) Neurobiology of craving, conditioned reward and relapse. Curr Opin Pharmacol 5:9–19

22. Bailey CP, Connor M (2005) Opioids: cellular mechanisms of tolerance and physical dependence. Curr Opin Pharmacol 5:60–68

23. Sharma SK, Klee WA, Nirenberg M (1977) Opiate-dependent modulation of adenylate cyclase. Proc Natl Acad Sci USA 74:3365–3369

24. Chakrabarti S, Wang L, Tang WJ et al (1998) Chronic morphine augments adenylyl cyclase phosphorylation: relevance to altered signaling during tolerance/dependence. Mol Pharmacol 54:949–953

25. Avidor-Reiss T, Nevo I, Levy R et al (1996) Chronic opioid treatment induces adenylyl cyclase V superactivation. Involvement of Gbetagamma. J Biol Chem 271:21309–21315

26. Houtani T, Nishi M, Takeshima H et al (2000) Distribution of nociceptin/orphanin FQ precursor protein and receptor in brain and spinal cord: a study using in situ hybridization and X-gal histochemistry in receptor-deficient mice. J Comp Neurol 424:489–508

27. Pan YX, Bolan E, Pasternak GW (2002) Dimerization of morphine and orphanin FQ/nociceptin receptors: generation of a novel opioid receptor subtype. Biochem Biophys Res Commun 297:659–663

28. Wang HL, Hsu CY, Huang PC et al (2005) Heterodimerization of opioid receptor-like 1 and mu-opioid receptors impairs the potency of micro receptor agonist. J Neurochem 92:1285–1294

29. Evans RM, You H, Hameed S et al (2010) Heterodimerization of ORL1 and opioid receptors and its consequences for N-type calcium channel regulation. J Biol Chem 285:1032–1040

30. Ueda H, Yamaguchi T, Tokuyama S et al (1997) Partial loss of tolerance liability to morphine analgesia in mice lacking the nociceptin receptor gene. Neurosci Lett 237:136–138

31. Ueda H, Inoue M, Takeshima H et al (2000) Enhanced spinal nociceptin receptor expression develops morphine tolerance and dependence. J Neurosci 20:7640–7647

32. Shaw G, Morse S, Ararat M et al (2002) Preferential transformation of human neuronal cells by human adenoviruses and the origin of HEK 293 cells. FASEB J 16:869–871

33. Chaturvedi K, Bandari P, Chinen N et al (2001) Proteasome involvement in agonist-induced down-regulation of mu and delta opioid receptors. J Biol Chem 276:12345–12355

34. Titus S, Neumann S, Zheng W et al (2008) Quantitative high-throughput screening using a live-cell cAMP assay identifies small-molecule agonists of the TSH receptor. J Biomol Screen 13:120–127

35. Gabriel D, Vernier M, Pfeifer MJ et al (2003) High throughput screening technologies for direct cyclic AMP measurement. Assay Drug Dev Technol 1:291–303

36. Jordan BA, Devi LA (1999) G-protein-coupled receptor heterodimerization modulates receptor function. Nature 399:697–700

37. Jenck F, Wichmann J, Dautzenberg FM et al (2000) A synthetic agonist at the orphanin FQ/nociceptin receptor ORL1: anxiolytic profile in the rat. Proc Natl Acad Sci USA 97:4938–4943

38. Avidor-Reiss T, Bayewitch M, Levy R et al (1995) Adenylyl-cyclase supersensitization in mu-opioid receptor-transfected Chinese hamster ovary cells following chronic opioid treatment. J Biol Chem 270:29732–29738

39. Gomes I, Jordan BA, Gupta A et al (2000) Heterodimerization of mu and delta opioid receptors: a role in opiate synergy. J Neurosci 20:RC110

40. Pfeiffer M, Koch T, Schroder H et al (2002) Heterodimerization of somatostatin and opioid receptors cross-modulates phosphorylation, internalization, and desensitization. J Biol Chem 277:19762–19772

41. Pfeiffer M, Kirscht S, Stumm R et al (2003) Heterodimerization of substance P and mu-opioid receptors regulates receptor trafficking and resensitization. J Biol Chem 278:51630–51637

42. Hojo M, Sudo Y, Ando Y et al (2008) mu-Opioid receptor forms a functional heterodimer with cannabinoid CB1 receptor: electrophysiological and FRET assay analysis. J Pharmacol Sci 108:308–319

43. Schroder H, Wu DF, Seifert A et al (2009) Allosteric modulation of metabotropic glutamate receptor 5 affects phosphorylation,

internalization, and desensitization of the micro-opioid receptor. Neuropharmacology 56:768–778

44. Walwyn W, John S, Maga M et al (2009) Delta receptors are required for full inhibitory coupling of mu-receptors to voltage-dependent Ca(2+) channels in dorsal root ganglion neurons. Mol Pharmacol 76:134–143

45. Law PY, Erickson-Herbrandson LJ, Zha QQ et al (2005) Heterodimerization of mu- and delta-opioid receptors occurs at the cell surface only and requires receptor-G protein interactions. J Biol Chem 280:11152–11164

46. Milligan G (2008) A day in the life of a G protein-coupled receptor: the contribution to function of G protein-coupled receptor dimerization. Br J Pharmacol 153(Suppl 1):S216–229

47. Chan JS, Chiu TT, Wong YH (1995) Activation of type II adenylyl cyclase by the cloned mu-opioid receptor: coupling to multiple G proteins. J Neurochem 65:2682–2689

48. Zhang S, Yu L (1995) Identification of dynorphins as endogenous ligands for an opioid receptor-like orphan receptor. J Biol Chem 270:22772–22776

49. Childers SR (1991) Opioid receptor-coupled second messenger systems. Life Sci 48:1991–2003

50. Meunier JC (1997) Nociceptin/orphanin FQ and the opioid receptor-like ORL1 receptor. Eur J Pharmacol 340:1–15

51. Duman RS, Tallman JF, Nestler EJ (1988) Acute and chronic opiate-regulation of adenylate cyclase in brain: specific effects in locus coeruleus. J Pharmacol Exp Ther 246:1033–1039

52. Simonds WF (1999) G protein regulation of adenylate cyclase. Trends Pharmacol Sci 20:66–73

53. Steiner D, Avidor-Reiss T, Schallmach E et al (2005) Regulation of adenylate cyclase type VIII splice variants by acute and chronic Gi/o-coupled receptor activation. Biochem J 386:341–348

54. Nestler EJ, Hope BT, Widnell KL (1993) Drug addiction: a model for the molecular basis of neural plasticity. Neuron 11:995–1006

55. Chan RY, Wong YH (1999) Chronic activation of ORL1 receptor induces supersensitization of adenylyl cyclase. Neuroreport 10:2901–2905

56. Tempel A, Zukin RS (1987) Neuroanatomical patterns of the mu, delta, and kappa opioid receptors of rat brain as determined by quantitative in vitro autoradiography. Proc Natl Acad Sci USA 84:4308–4312

57. Fukuda K, Kato S, Mori K et al (1994) cDNA cloning and regional distribution of a novel member of the opioid receptor family. FEBS Lett 343:42–46

58. Lane-Ladd SB, Pineda J, Boundy VA et al (1997) CREB (cAMP response element-binding protein) in the locus coeruleus: biochemical, physiological, and behavioral evidence for a role in opiate dependence. J Neurosci 17:7890–7901

59. Zachariou V, Liu R, LaPlant Q et al (2008) Distinct roles of adenylyl cyclases 1 and 8 in opiate dependence: behavioral, electrophysiological, and molecular studies. Biol Psychiatry 63:1013–1021

60. Han MH, Bolanos CA, Green TA et al (2006) Role of cAMP response element-binding protein in the rat locus ceruleus: regulation of neuronal activity and opiate withdrawal behaviors. J Neurosci 26:4624–4629

61. Cao JL, Vialou VF, Lobo MK et al (2010) Essential role of the cAMP–cAMP response-element binding protein pathway in opiate-induced homeostatic adaptations of locus coeruleus neurons. Proc Natl Acad Sci U S A 107:17011–17016

62. Mogil JS, Grisel JE, Reinscheid RK et al (1996) Orphanin FQ is a functional anti-opioid peptide. Neuroscience 75:333–337

63. Shoblock JR, Wichmann J, Maidment NT (2005) The effect of a systemically active ORL-1 agonist, Ro 64–6198, on the acquisition, expression, extinction, and reinstatement of morphine conditioned place preference. Neuropharmacology 49:439–446

64. Marquez P, Nguyen AT, Hamid A et al (2008) The endogenous OFQ/N/ORL-1 receptor system regulates the rewarding effects of acute cocaine. Neuropharmacology 54:564–568

65. Kotlinska J, Rafalski P, Biala G et al (2003) Nociceptin inhibits acquisition of amphetamine-induced place preference and sensitization to stereotypy in rats. Eur J Pharmacol 474:233–239

66. Heishman SJ, Stitzer ML, Bigelow GE et al (1989) Acute opioid physical dependence in postaddict humans: naloxone dose effects after brief morphine exposure. J Pharmacol Exp Ther 248:127–134